remote sensing

MDPI

Article

Estimation of Malondialdehyde Content in *Medicago truncatula* Under Salt Stress Based on Multi-Order Spectral Transformation Characteristics

Jiaxin Zhang [1,2,3], Jingyu Zhang [4], Juan Wang [1,2,3], Aiwu Zhang [1,2,3,*] and Xiong Deng [4]

1 Key Laboratory of 3D Information Acquisition and Application, Ministry of Education, Capital Normal University, Beijing 100048, China; jxzhang@cnu.edu.cn (J.Z.); 2230901020@cnu.edu.cn (J.W.)
2 Engineering Research Center of Spatial Information Technology, Ministry of Education, Capital Normal University, Beijing 100048, China
3 Center for Geographic Environment Research and Education, College of Resource Environment and Tourism, Capital Normal University, Beijing 100048, China
4 Key Laboratory of Plant Molecular Physiology, Institute of Botany, Chinese Academy of Sciences, Beijing 100093, China; jingyuzhang@ibcas.ac.cn (J.Z.); dengxiongred@163.com (X.D.)
* Correspondence: zhangaiwu@cnu.edu.cn

Abstract: Salt stress is a significant abiotic factor affecting the growth and development of alfalfa. Malondialdehyde (MDA) serves as a critical biomarker for assessing alfalfa's salt tolerance. Traditional methods for measuring MDA are often time-consuming and labor-intensive. Recent advances in remote sensing technology have made non-destructive estimation of metabolites feasible, positioning the accurate estimation of MDA content in alfalfa as a key focus in intelligent breeding. To address the challenge of detecting subtle changes in MDA content, this study developed a partial least squares regression (PLSR) model specifically for *Medicago truncatula*. This study utilized leaf reflectance hyperspectral data across the visible near-infrared–shortwave infrared (VIR-NIR-SWIR) spectrum, applying multi-order spectral transformation methods, including continuous wavelet transform (CWT), fractional differential (FD), and multi-granularity spectral segmentation (MGSS). Feature selection techniques, such as sequential forward selection (SFS), Least-Squares Boosting (LSBoost), and feature selection using neighborhood component analysis for regression (FSRNCA), were employed to enhance the efficiency of the MDA estimation. The findings revealed that the optimal PLSR model for MDA estimation was achieved by integrating CWT features across orders 1–30 with the SFS method. This model demonstrated robust estimation capabilities under varying salt stress conditions, significantly outperforming the original spectral data (R^2 = 0.654, RMSE = 22.567 vs. R^2 = 0.242, RMSE = 33.411). A comparative analysis of feature selection methods confirmed that SFS was the most effective for estimating MDA content in alfalfa. These results provide valuable insights and methodologies for MDA estimation and evaluating salt tolerance in alfalfa.

Keywords: hyperspectral data; spectral transformation; malonaldehyde; multi-order combination; sequential forward selection

check for updates

Citation: Zhang, J.; Zhang, J.; Wang, J.; Zhang, A.; Deng, X. Estimation of Malondialdehyde Content in *Medicago truncatula* Under Salt Stress Based on Multi-Order Spectral Transformation Characteristics. *Remote Sens.* **2024**, *16*, 4049. https://doi.org/10.3390/rs16214049

Academic Editor: Clement Atzberger

Received: 9 August 2024
Revised: 24 October 2024
Accepted: 29 October 2024
Published: 30 October 2024

Correction Statement: This article has been republished with a minor change. The change does not affect the scientific content of the article and further details are available within the backmatter of the website version of this article.

Copyright: © 2024 by the authors. Licensee MDPI, Basel, Switzerland. This article is an open access article distributed under the terms and conditions of the Creative Commons Attribution (CC BY) license (https://creativecommons.org/licenses/by/4.0/).

1. Introduction

Alfalfa is a crucial feed source for animal husbandry, but the expansion of saline land in recent years has significantly hindered its growth and development, negatively impacting its quality [1–3]. Malondialdehyde (MDA) is a metabolite that serves as a key indicator of alfalfa's salt tolerance. It plays a vital regulatory role in various physiological processes, including photosynthesis, maintaining cell membrane integrity, and resistance to environmental stressors [4,5]. Consequently, the accurate and rapid estimation of MDA concentrations in alfalfa is essential for understanding its physiological functions and evaluating its overall health [6].

MDA is produced through lipid peroxidation in plant tissues or organs in response to oxidative stress during various environmental stresses or aging processes. Higher MDA levels correlate with greater plant damage, as confirmed in studies examining plant responses to abiotic and biotic stresses [7,8]. Therefore, MDA content serves as a reliable marker for assessing plant growth dynamics under stress. By predicting MDA levels, it is possible to gauge the extent of injury in stressed plants, allowing for the implementation of appropriate stress mitigation strategies [5,9].

The Thiobarbituric Acid (TBA) method is the most commonly used technique for measuring MDA content in plants. However, this method is time-consuming, labor-intensive, and prone to interference from other substances. Its destructive nature and lengthy procedures make it unsuitable for the real-time monitoring of MDA dynamics. Furthermore, the TBA method requires stringent experimental conditions and sample integrity, which limits its practical application [10]. Given these challenges, there is an urgent need to develop non-destructive, rapid, accurate, and cost-effective methods for measuring MDA content, catering to the needs of plant physiological research and agricultural production. In recent years, remote sensing technology has advanced rapidly and is increasingly being applied to plant physiological studies [11]. Despite these advancements, the accurate and efficient monitoring of MDA content remains constrained by several limitations.

Hyperspectral techniques in the visible to shortwave infrared range are essential for advancing research on alfalfa metabolite estimation [12]. However, most studies on non-destructive metabolite estimation have primarily focused on the near-infrared region, with limited exploration of hyperspectral and multispectral spectra [13,14]. For example, Zhang combined near-infrared spectroscopy with PLSR to rapidly measure MDA content in slash pine and loblolly pine under drought stress using various spectral preprocessing and feature selection methods. The established optimal PLS model is capable of reliably and non-destructively detecting MDA levels in real time [4]. Kong utilized hyperspectral imaging in the 400–1000 nm range to assess MDA content in oilseed rape leaves under herbicide stress, achieving a correlation coefficient (RP) of 0.929 and a root mean square error of prediction (RMSEP) of 2.951 [13]. Similarly, Chen studied Cabernet Sauvignon grapes at various ripening stages and developed a prediction model for anthocyanin and total phenol content in grape skins using hyperspectral imaging and multiple regression within the 900–1700 nm range. This approach enabled the non-destructive and efficient detection of phenolic content, offering a new method for phenolic detection in ripening wine grapes [15]. Additionally, Cen developed a hyperspectral estimation model for flavonoids and polysaccharides in goldenseal using an empirical model, showing similar accuracy between the trained and tested models. This study further validated the feasibility of using hyperspectral non-destructive monitoring techniques for metabolite estimation [16].

Despite these advancements, challenges remain in accurately estimating MDA content, as hyperspectral imaging often fails to capture subtle physiological and biochemical changes in plants [17]. Multi-order spectral transform technology will be a breakthrough in plant physiology and biochemistry monitoring research. Commonly used spectral transform methods include multi-order CWT [18,19] and FD [20], as well as a new method called MGSS [21,22]. FD is an extension of integer order differential, which has achieved certain results in the application of soil organic matter content [23], soybean canopy nitrogen content [24], chlorophyll content [25], and so on. CWT is a transformation of the original spectrum in the spectral domain. In recent years, it has been used in hyperspectral inversion modeling and has been well verified in the estimation of soil organic carbon [26]. MGSS is a new method derived by Kang based on the high-order binary coding method of the spectrum [27]. The high-performance estimation of the crude protein content of natural grassland grass by hyperspectral image is realized by using the MGSS technology system. On this basis, the weakly sensitive characteristics related to biomass, physical and chemical parameters, and nutrient content were extracted, and the estimation accuracy was improved to more than 0.78 [21,22]. Xiang extended the MGSS technology to the monitoring of soil salinity, effectively extracted the weakly spectral information in the soil,

and expanded the range of spectral utilization. In summary, from the existing research, it is found that the weak spectral information of the original spectrum can be extracted by spectral transformation, thereby enhancing the ability of hyperspectral to capture detailed information [28,29].

Multi-order spectral transformation technology provides a significant advantage over traditional spectral analysis by extracting richer spectral information and enhancing the signals related to MDA content in plant tissues. This method enables a more accurate reflection of physiological changes by interacting with various chemical components [30,31]. However, challenges remain in estimating MDA content in plants. Most existing studies primarily focus on the near-infrared region, overlooking the full potential of the visible spectrum and other wavelengths. Although the literature acknowledges the promise of multi-order spectral transformation for MDA estimation, research in this area is still limited. The implicit information within multi-order spectral characteristics is underexplored, and factors such as environmental conditions, plant species, and growth stages introduce further complexity to the estimation models.

The purpose of this study was to develop a method for estimating MDA content in alfalfa leaves using VIR-SWIR spectroscopy combined with multi-order spectral transformation characteristics. This approach aims to overcome the limitations of existing methods and enhance the accuracy and reliability of estimation results. Specifically, we focused on the potential of integrating multi-order combinations of MGSS, FD, CWT, and other techniques for estimating MDA content in alfalfa. Additionally, we incorporated feature selection methods to establish a robust quantitative analysis model. The objectives of this study are as follows: (1) To develop a reliable technique for estimating and predicting MDA content in alfalfa under various salt stress conditions by integrating multi-order spectral transformation features; and (2) To investigate the influence of different spectral transformation methods, diverse feature selection techniques, and varying levels of MDA content on the estimation process. The findings of this study will provide new methods and tools for accurately estimating MDA content and offer a scientific basis for understanding the role of MDA in physiological processes, as well as assessing the health status of alfalfa.

2. Materials and Methods

2.1. Experimental Area and Design

This experiment was conducted in the greenhouse facilities of the Institute of Botany, Chinese Academy of Sciences, with the *Medicago truncatula* ecotype Jemalong A17.

To establish a comprehensive MDA content status system under various salt stress conditions for the purpose of enhancing the generality of the estimation model, all the materials were randomly divided into four groups, each consisting of 60 plants. After normal cultivation for 30 days, the four groups were subjected to salt treatments at concentrations of 0, 100, 200, and 250 mmol/L, respectively. Subsequently, leaf spectral reflectance curves were collected from the different treatment groups on days 1, 3, and 5 (Figure 1).

2.2. Data Acquisition and Preprocessing

The data obtained in this study consist of two components: hyperspectral data and MDA data. The hyperspectral data were acquired using the ASD Field Spec 4 portable spectroradiometer. This spectral dataset has 2150 contiguous narrow bands, covering the spectral range from VIR to SWIR (350–2500 nm). The measurement procedures followed the instrument's user manual and included preheating and spectral correction. Given the relatively small size of *Medicago truncatula* leaves, leaf clips with bifurcated optical fibers and a 5-watt halogen lamp light source were utilized to obtain accurate reflectance curves. To ensure that the leaf samples accurately represented the salt stress conditions of *Medicago truncatula*, three types of leaves (young leaves, old leaves, and intermediate leaves) were selected from each plant, with approximately 8 leaves from each leaf type being measured. After obtaining the spectral curves, any curves displaying significant error were analyzed

and removed. Subsequently, the remaining curves were averaged to generate the spectral reflectance curve for each *Medicago truncatula* plant.

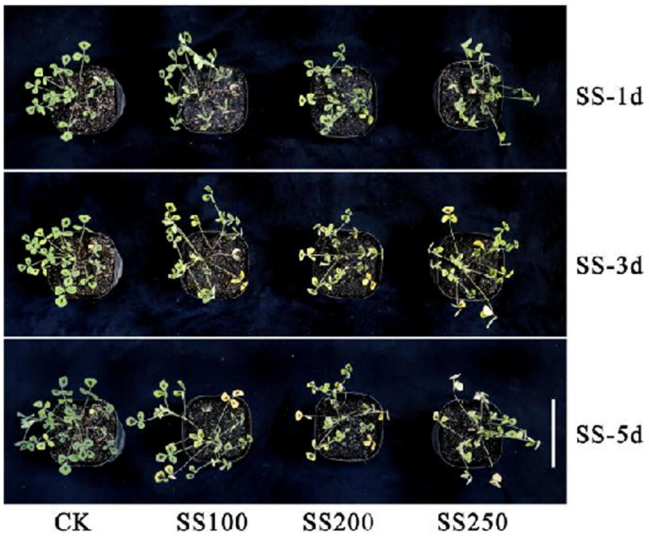


Figure 1. Growth diagram of alfalfa under different treatments. CK is the control group, SS is the salt stress group, SS100 represents the salt concentration of the stress group of 100 mmol/L, SS-1d represents the first day of alfalfa growth diagram.

To measure the MDA content in the *Medicago truncatula* leaves, immediately after acquiring the spectral curves, the leaves were frozen at −2 °C. Subsequently, the MDA content was measured using the kit provided by Suzhou Keming Science and Technology Co., Ltd. (Suzhou, China). Three biological replicates were utilized to minimize experimental errors, and the significance of the difference passed the statistical t test. The sample histogram is shown in Figure 2.

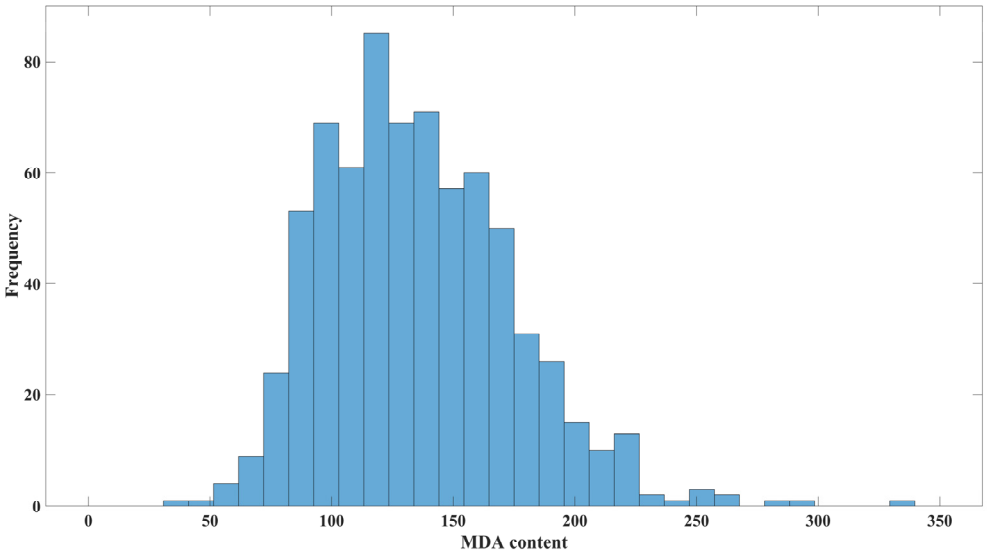


Figure 2. Histogram distribution of malondialdehyde content in samples.

2.3. Methods

To construct a model for estimating MDA content, the process involves five main components, as illustrated in Figure 3. (1) Multi-order spectral transformation (Section 2.3.1): This step involves calculating three types of multi-order spectral transformation features from the original spectrum, including CWT, FD, and MGSS, where CWT and MGSS features

were extracted from order 1–30, and FD features were extracted from order 1–20. (2) Feature selection (Section 2.3.2): In this paper, the spectral transform features of different orders and multi-order combinations were firstly considered in the spectral analysis, in which the spectral transform features of different orders were combined for different orders of three spectral transform features, respectively, and the spectral transform features of multi-order combinations were obtained by combining all the orders of three spectral transform features, respectively. Then, three feature selection methods were carried out for different orders and multi-order combinations of different spectral transform features, respectively, including the sequential forward selection (SFS), feature selection using neighborhood component analysis (FSRNCA), and LSBoost methods. (3) Model construction (Sections 2.3.3 and 2.3.4): Using the features selected in step 2, PLSR models were constructed for estimating MDA content. The performance of the models was evaluated by calculating R^2 and RMSE for both training and testing datasets. (4) Analysis of results (Section 3): Based on the estimation results using different order spectral transformation features, an analysis was conducted to investigate the impact of spectral transformation features, feature selection methods, and MDA content on estimation accuracy. Additionally, the results obtained from multi-order combination spectral transformation features are explored to identify the advantages of using multi-order combinations for estimation accuracy; the distribution of features in the optimal model is also analyzed.

2.3.1. Multi-Order Spectral Transformation

Hyperspectral data contain rich band information, which can help to capture the physiological and biochemical changes in alfalfa. However, they still fall short in capturing detailed information about the plants. Spectral transformation, by mathematically transforming and processing the original hyperspectral data, is highly sensitive to specific phenotypic attributes and physiological processes, and helps to improve the accuracy of MDA content estimation. Multi-order CWT and FD are commonly used multi-order spectral transform methods. MGSS is a new method based on the spectral HOBC method [21,27]. The multi-order information extraction technology can expand the original 1-dimensional spectrum to n-dimensional and quantify the alfalfa parameter information with different order features. These three algorithms can achieve the purpose of mining weak spectral information and improving the separability of the spectrum.

The MGSS method is used to extract spectral information and highlight the weak spectral information. In this paper, the MGSS features were extracted from 30 orders in the range of 1–30 (Figure 4, Formulas (1) and (2)).

$$V = \sum_{i=1}^{M} \beta_i H_i + R_M(V) \approx \sum_{i=1}^{M} \beta_i H_i \tag{1}$$

Here, H_i is the i-order binary code vector of vector V; β_i is the coefficient of H_i and $\beta_i > 0$; and $R_M(V)$ is the residual vector of M-order quantized estimation of V.

$$\begin{cases} SF_i = SF_{i-1} - SL_i \\ SL_i = \beta_i * H_i \\ AS_i = \sum_{t=1}^{i} SL_t \end{cases} \tag{2}$$

SF_i is the segmentation feature (SF) after the i-th spectral segmentation. SL_i is the baseline for the i-th SF segmentation. AS_i is the approximate spectrum after the i-th spectral segmentation, and also contains the MGSS features used to construct the MDA estimation model in this paper. Its essence is to gradually approximate the original hyperspectral by continuously accumulating from the segmentation values.

Multi-order CWT extracts key features from plant hyperspectral data by enhancing subtle variations in specific frequency ranges or spectral scales of the signal. By selecting appropriate wavelet basis functions and scale parameters, localized details in plant

spectral curves and frequency components related to alfalfa growth can be highlighted, thus enhancing useful information in plant hyperspectral data. In this study, the Symlets wavelet basis function and a scale analysis range of 1–30 were used. The Symlets wavelet is a wavelet function based on polynomial approximation (Figure 5, Formulas (3) and (4)). In plant hyperspectral curves, trends and variations can be captured through polynomial approximation. By utilizing multiple scales or spectral resolutions, the spectral curves can be analyzed across different frequency ranges, thereby obtaining features from various frequency ranges.

$$W_f(a,b) = \langle x(\beta), \psi_{a,b}(\beta) \rangle = \int_{-\infty}^{+\infty} x(\beta)\psi_{a,b}(\beta)d(\beta) \tag{3}$$

$$\psi_{a,b}(\beta) = \frac{1}{\sqrt{a}}\phi\left(\frac{\beta - b}{a}\right) \tag{4}$$

Here, $W_f(a,b)$ is the wavelet coefficient; $x(\beta)$ is the spectral reflectance in the β band, $\beta = 1, 2, 3, \ldots, n$; n is the number of hyperspectral bands; and $\psi_{a,b}(\beta)$ is the wavelet basis functions with scale factor a and translation factor b.

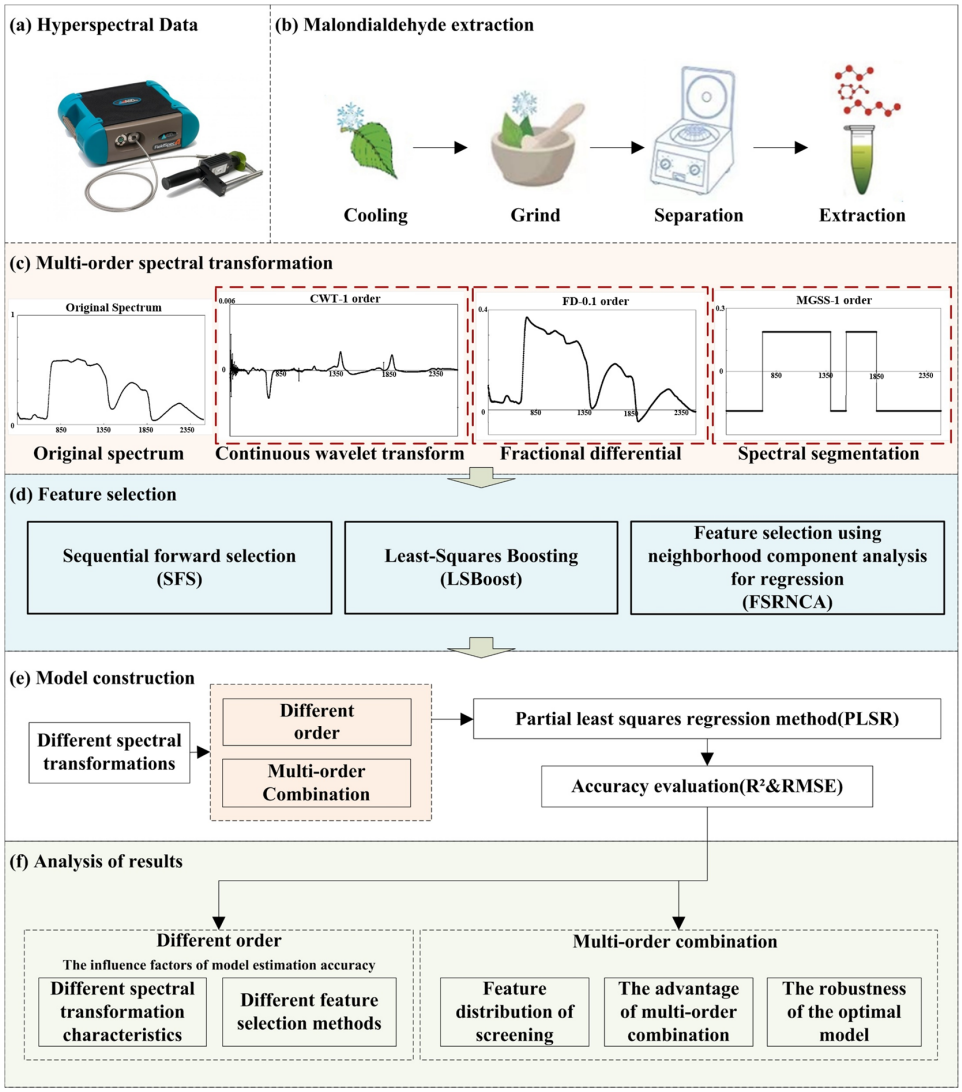


Figure 3. A workflow diagram of the experimental design, feature extraction, and modeling. (**a**) Hyperspectral data; (**b**) Malondialdehyde extraction; (**c**) Multi-order spectral transformation; (**d**) Feature selection; (**e**) Model construction; (**f**) Analysis of results.



Figure 4. Example plot of multi-granularity spectral segmentation features.

Multi-order FD is an extension of integer-order differential, and it is also one of the most commonly used spectral transformation methods in recent years. It can make up for the data loss problem caused by integer-order differential transformation. The algorithm has been applied to soil chemical element content, water nitrogen concentration, chlorophyll estimation, and other fields to improve the estimation accuracy of the target. In this paper, 20 order results in the range of 0.1–2 were analyzed with 1 as the step size and 0.1 as the arithmetic interval (Figure 6, Formulas (5)–(7)).

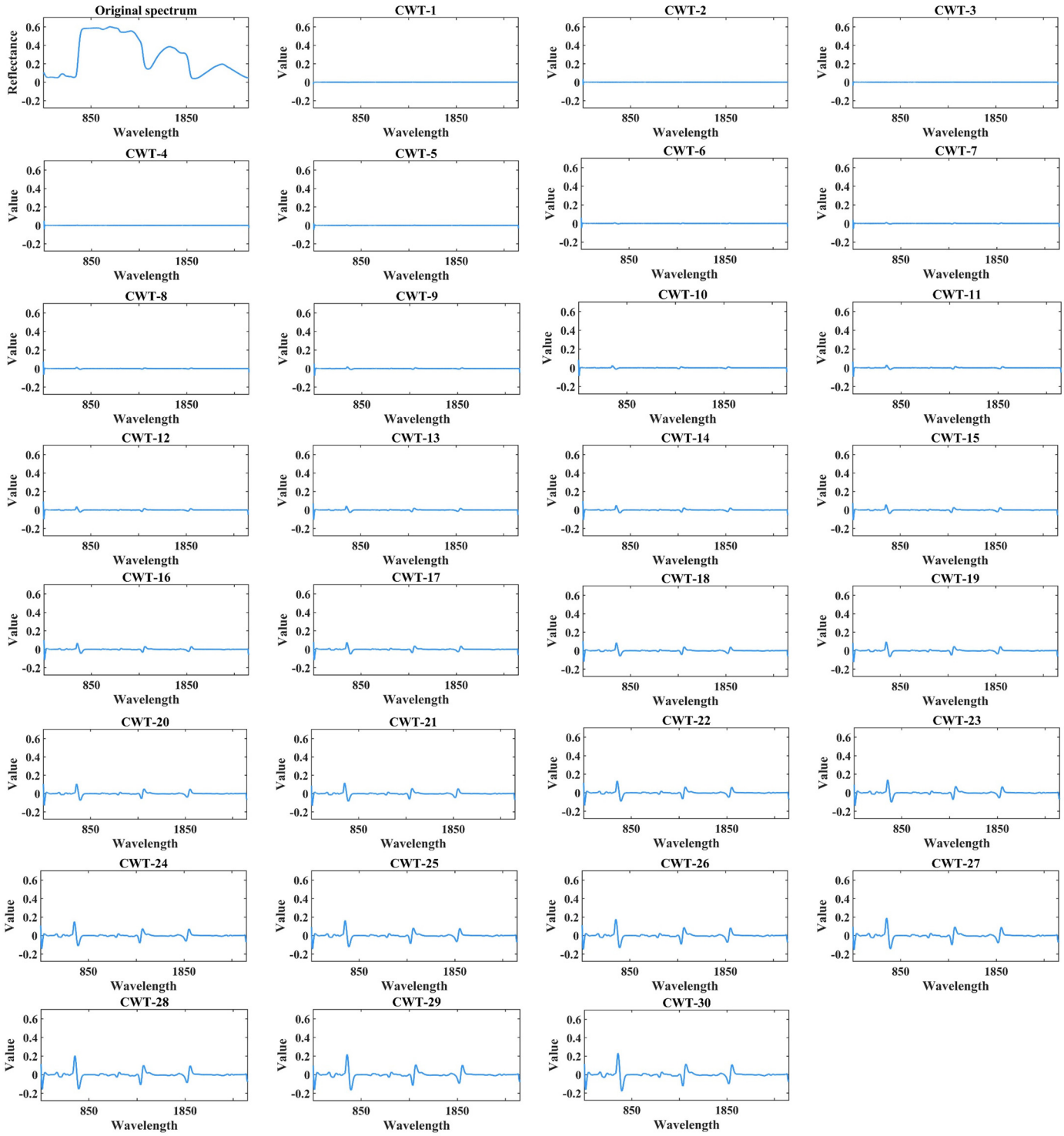


Figure 5. Example plot of multi-order continuous wavelet transform features.

$$d^v f(x) = \lim_{h \to 0} \frac{1}{h^v} \sum_{m=0}^{\frac{t-p}{h}} (-1)^m \frac{\Gamma(v+1)}{m!\Gamma(v-m+1)} f(x-mh) \tag{5}$$

$$\Gamma(z) = \int_0^{\infty} e^{-u} u^{z-1} du = (z-1)! \tag{6}$$

where x is the spectral reflectance; v is the spectral transformation order; h is the differentiation step; and t and p denote the upper and lower limits of the differentiation, respectively.

$\Gamma(*)$ is the Gamma function, and if the spectral spacing is resampled to 1 nm ($h = 1$), the formula can be further simplified as:

$$\frac{d^v f(x)}{dx^v} \approx f(x) + (-v)f(x-1) + \frac{(-v)(-v+1)}{2} f(x-2) + \ldots + \frac{\Gamma(-v+1)}{n!\Gamma(-v+n+1)} f(x-n) \quad (7)$$

where n is the difference between the upper and lower differential limits, and if $v = 0$, it denotes the function itself.

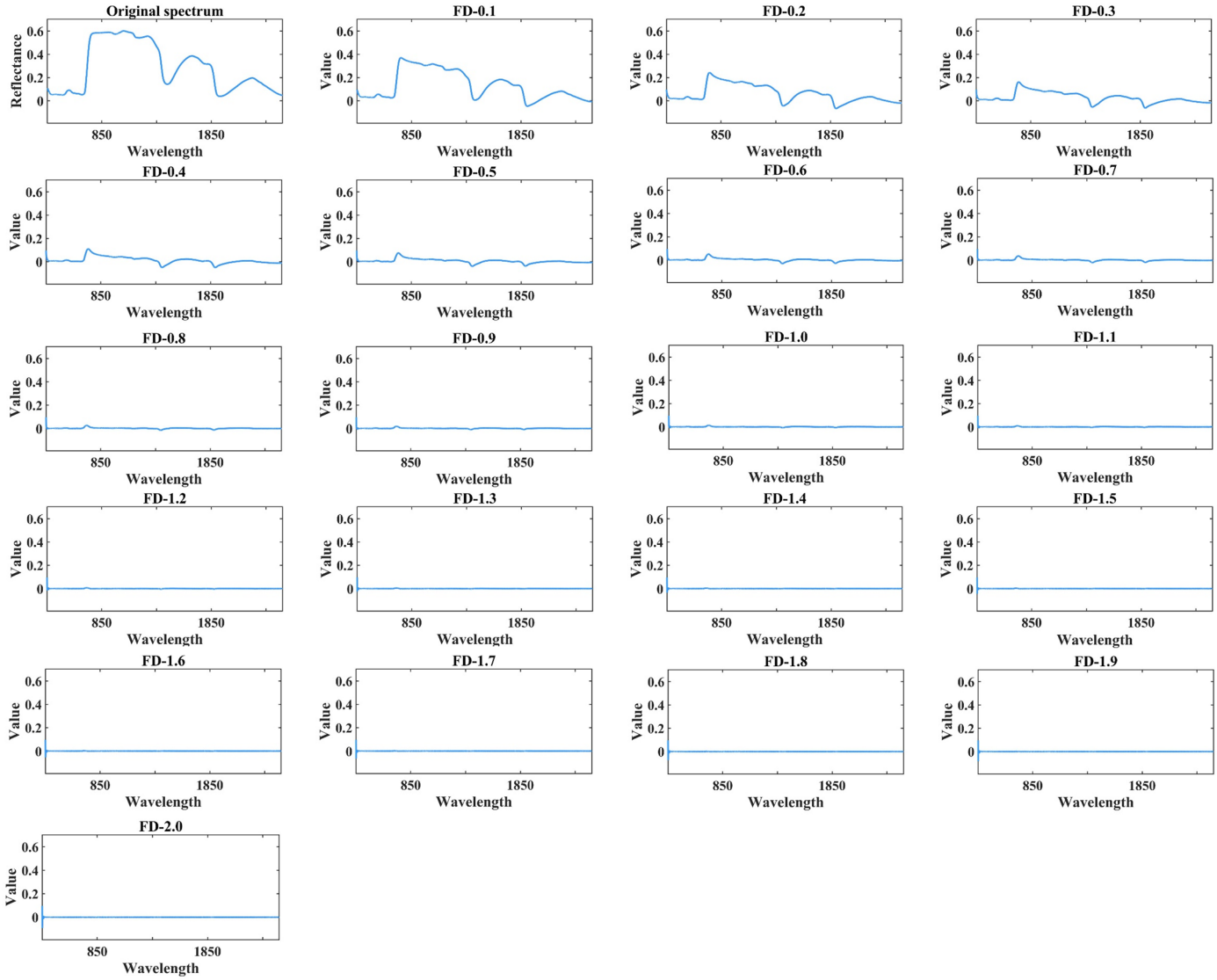


Figure 6. Example plot of multi-order fractional differential features.

2.3.2. Feature Selection

Hyperspectral narrow-wave spectra and their multi-order spectral transform features have many features with redundant or useless information, and at the same time, the number of samples was much smaller than the spectral features, which increases the risk of overfitting the model. Removing irrelevant features can reduce the model complexity, increase its interpretability, and enhance the stability of the model effect. Therefore, it is necessary to perform feature selection when constructing the estimation model. The SFS, FSRNCA, and LSBoost methods are commonly used feature selection methods.

SFS is a method that gradually adds unselected features to an initial set of features to build a model with optimal performance. In each step, features that can bring about an improvement in model performance are selected until a preset number of features is reached, and then stopped. SFS improves the predictive ability and generalization performance of the model by constructing a simple and accurate model, but it may not always be able to find the globally optimal subset of features due to the influence of the correlation between the features. Through testing, this paper set the number of features at 15, 30, 45, 60, 75, and 90 to construct the model, respectively, and then selected the optimal result.

LSBoost is an integrated learning method based on gradient boosting for solving regression problems. The initial model is a constant, and the loss function is made smaller by adding new base learners in a gradual and iterative manner to achieve accurate prediction on the regression problem. LSBoost is able to capture complex nonlinear relationships, but the method is sensitive to outliers, and overfitting may occur when the learning rate is too high or the number of base learners is too large. Through testing, this paper set the number of features at 100, 300, 500, 700, 900, and 1100 to construct the model, respectively, and then selected the optimal results.

FSRNCA maximizes the probability of similar samples and optimizes the distance metric by mapping the original features into a new low-dimensional space, thus improving the model performance in the regression task. The FSRNCA method takes into account the relationships between similar samples when learning the mapping, so that the mapping is more adapted to the distribution and structure of the data, and thus better captures the associations between the samples in the regression problem. Through testing, this paper set the number of features at 100, 300, 500, 700, 900, and 1100 to construct the model, respectively, and then selected the optimal results.

In this paper, the different order features of the three spectral transform features as well as the multi-order combination of the features are, respectively, feature selected and an estimation model is established, on the basis of which the influence of the estimation model of the different order features is explored, as well as the advantages of the multi-order combination in the estimation of MDA.

2.3.3. Model Construction

In this study, the number of samples is much smaller than the number of independent variables. PLSR is more interpretable in spectral analysis, effectively reduces the feature space, and addresses the issue of covariance. Therefore, it is a more suitable regression modeling method for this study [32]. Based on the method of Section 2.3.2, features of different orders and all order combinations were selected as independent variables, while MDA content was used as the dependent variable. The PLSR method was used to establish a model for estimating the MDA content of alfalfa, with all processes implemented using Matlab R2019b.

In the modeling process, when choosing fewer principal components, the model may suffer from underfitting, as too few principal components cannot adequately reflect the spectral variations of the components to be measured in the samples. Conversely, selecting too many principal components may lead to overfitting, which results in the inclusion of certain principal components representing noise in the model, thereby reducing the model's accuracy and predictive ability. To address these challenges, we set the cumulative contribution of the principal components at 0.95 and selected the number of principal components adaptively. The default parameters for the PLSR model included the following: the number of components (ncomp) was determined through cross-validation; the NIPALS algorithm was employed as the computation method; 10-fold cross-validation was conducted; the maximum iterations (MaxIter) were set to 100; and the convergence tolerance (TolFun) was maintained at a default value of 1×10^{-6} to ensure model convergence. This approach aimed to reduce overfitting and underfitting phenomena while ensuring that the estimation model captures a substantial amount of information.

2.3.4. Precision Validation

All combinations of the features extracted in Section 2.3.2 were combined with MDA to build the estimation model described in Section 2.3.3. For each dataset, 70% (504) of the data were extracted for training and the remaining 30% (216) were tested.

The coefficient of determination (R^2) and root mean square error (RMSE) were used as model evaluation criteria to select the best prediction model, and to estimate the contribution of each factor to the estimation of MDA.

3. Results

3.1. The Relationship between Spectral Transformation Characteristics and MDA Content

The correlations of the original spectrum and MGSS characteristics with MDA content and their correlation frequency distributions were significantly different (Figure 7). The correlation coefficients (absolute value, same below) between the original spectrum and MDA content were mostly distributed between 0.1 and 0.2. The correlation coefficients between the MGSS characteristics and MDA content were similar, but the number of bands with correlation coefficients in the 0.2–0.3 range had increased compared to the original spectrum. The MGSS characteristics obviously enhanced the correlation between the SWIR and MDA content from the 4th order. Overall, the MGSS characteristics increased the number of bands with larger correlation coefficients. Combining Figures 4 and 7, it could be found that the curve waveforms and correlation coefficient tend to stabilize after the 7th order MGSS.

Comparing the correlation coefficients between the original spectrum and the multi-order CWT characteristics and MDA content (Figure 8), we found that the number of bands with correlations of 0.2 or more between the CWT characteristics and MDA content was significantly greater than that of the original spectrum. As the CWT characteristics order increased, the characteristics shifted from being mostly distributed in the 0–0.1 interval to the 0.1–0.4 interval, significantly boosting the number of bands with larger correlation coefficients with MDA content. Combining Figures 5 and 8, it can be found that the waveforms of CWT characteristics of different orders were different, but their correlation distribution was stable after the 15th order.

Comparing the correlation coefficient and frequency diagram between the original spectrum and multi-order FD characteristics and MDA content (Figure 9), it could be seen that the overall distribution of the correlation coefficient between FD the characteristics and MDA content changed with the increase in order, and the number of features with a correlation coefficient above 0.2 showed a trend of increasing first and then decreasing. Combining Figures 6 and 9, it could be found that the waveform of fractional differential characteristics tended to be gentle as the order went up.

3.2. Feature Distribution

In this paper, three spectral transform features, 1–30th order MGSS, 1–20th order FD, and 1–30th order CWT of the original spectrum were calculated, and then the feature screening of the original spectrum and three spectral transform order-by-order features were carried out based on the SFS method, the LSBoost method, and the FSRNCA method, respectively (Figure 10 and Table 1). Secondly, the feature screening of these three spectral transform combination features was carried out based on the SFS, LSBoost, and FSRNCA methods for the combined features of these three spectral transforms (Figure 11 and Table 2), and we then established the estimation model.

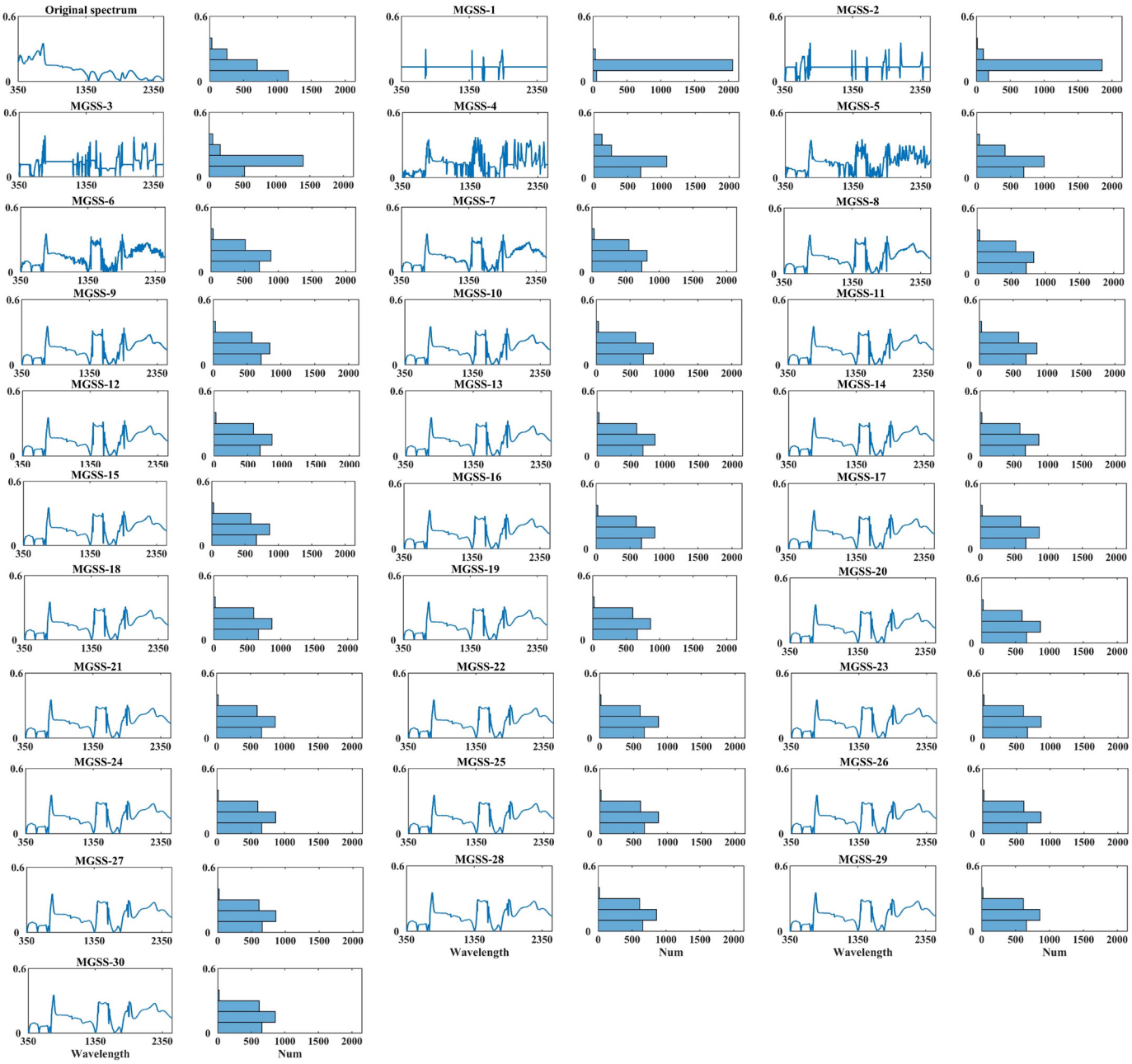


Figure 7. Pearson correlation coefficients (absolute values) of original spectrum and 1–30 order spectral segmentation features with malondialdehyde content and their frequency plots.

Table 1. The results of different order alfalfa malondialdehyde estimation model.

Methods	SFS				LSBoost				FSRNCA			
Characteristics	Train		Test		Train		Test		Train		Test	
	R^2	RMSE	R^2	RMSE	R^2	RMSE	R^2	RMSE	R^2	RMSE	R^2	RMSE
Original	0.242	34.678	0.236	33.563	0.273	33.964	0.204	34.258	0.245	34.599	0.242	33.411
MGSS-5	0.438	29.854	0.080	36.824	0.381	31.340	0.157	35.248	0.358	31.898	0.096	40.323
MGSS-10	0.348	32.165	0.201	34.316	0.271	34.008	0.258	33.076	0.352	32.049	0.071	40.878
MGSS-15	0.268	34.074	0.198	34.374	0.344	32.248	0.231	33.668	0.318	32.890	0.113	39.950
MGSS-20	0.326	32.685	0.189	34.562	0.355	31.980	0.219	33.918	0.308	33.138	0.124	39.701

Table 1. *Cont.*

Methods	SFS				LSBoost				FSRNCA			
Characteristics	Train		Test		Train		Test		Train		Test	
	R^2	RMSE	R^2	RMSE	R^2	RMSE	R^2	RMSE	R^2	RMSE	R^2	RMSE
FD-0.5	0.253	34.427	0.214	34.040	0.314	32.981	0.195	34.441	0.291	33.528	0.172	38.599
FD-1.0	0.401	30.815	0.305	32.000	0.319	32.873	0.268	32.848	0.209	35.407	0.089	40.496
FD-1.5	0.411	30.557	0.329	31.451	0.360	31.848	0.370	30.465	0.307	33.160	0.077	40.748
FD-2.0	0.421	30.303	0.323	31.575	0.288	33.609	0.242	33.429	0.276	33.882	0.088	40.503
CWT-5	0.405	30.724	0.315	31.779	0.386	31.203	0.398	29.783	0.376	31.458	0.145	39.225
CWT-10	0.527	27.394	0.411	29.471	0.360	31.855	0.384	30.140	0.298	33.354	0.212	37.663
CWT-15	0.542	26.948	0.425	29.098	0.387	31.174	0.387	30.047	0.282	33.748	0.189	38.210
CWT-20	0.480	28.707	0.430	28.991	0.332	32.548	0.251	33.233	0.289	33.576	0.179	38.433

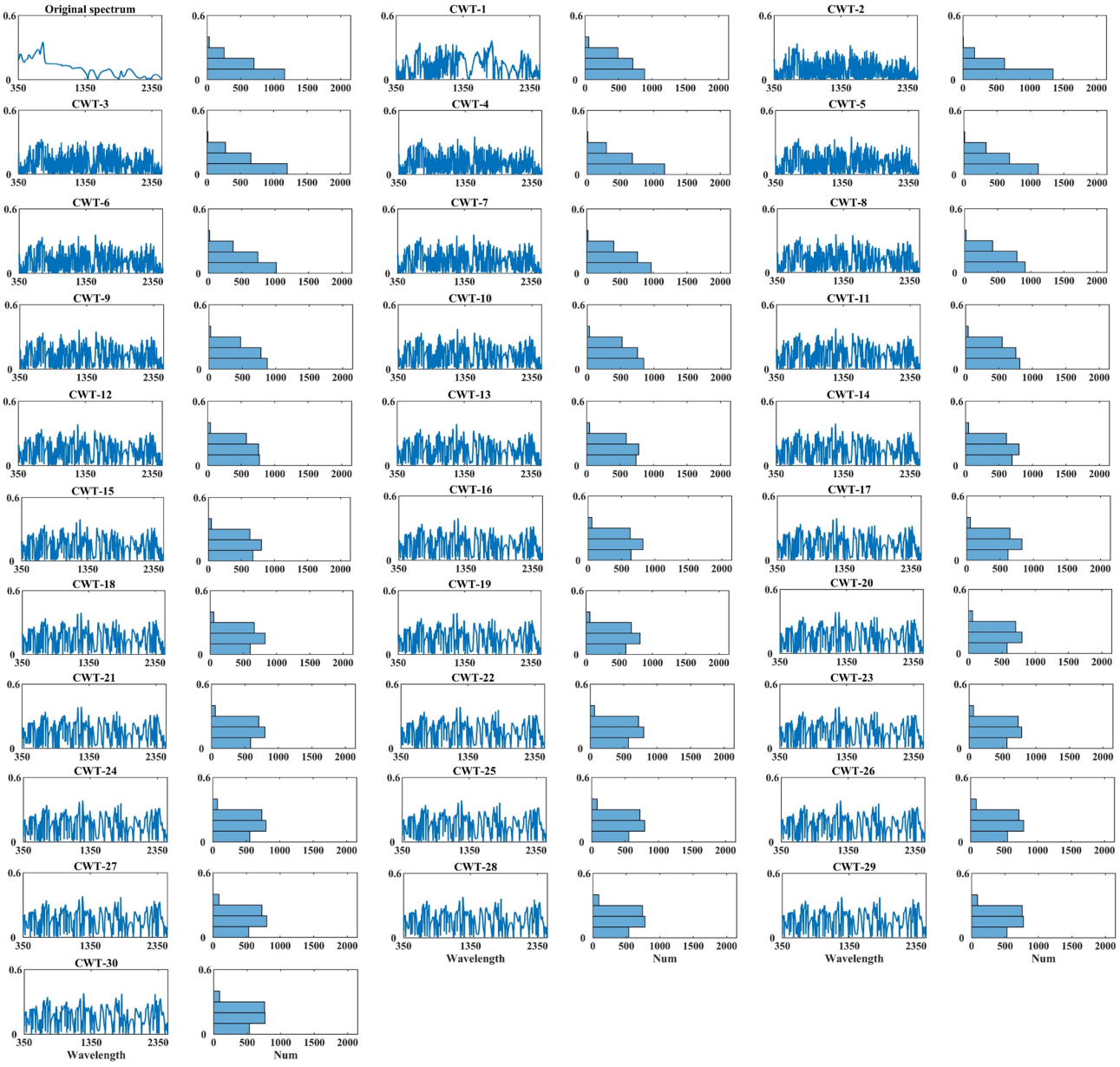


Figure 8. Pearson correlation coefficients (absolute values) of original spectrum and 1–30 order continuous wavelet transform features with malondialdehyde content and their frequency plots.

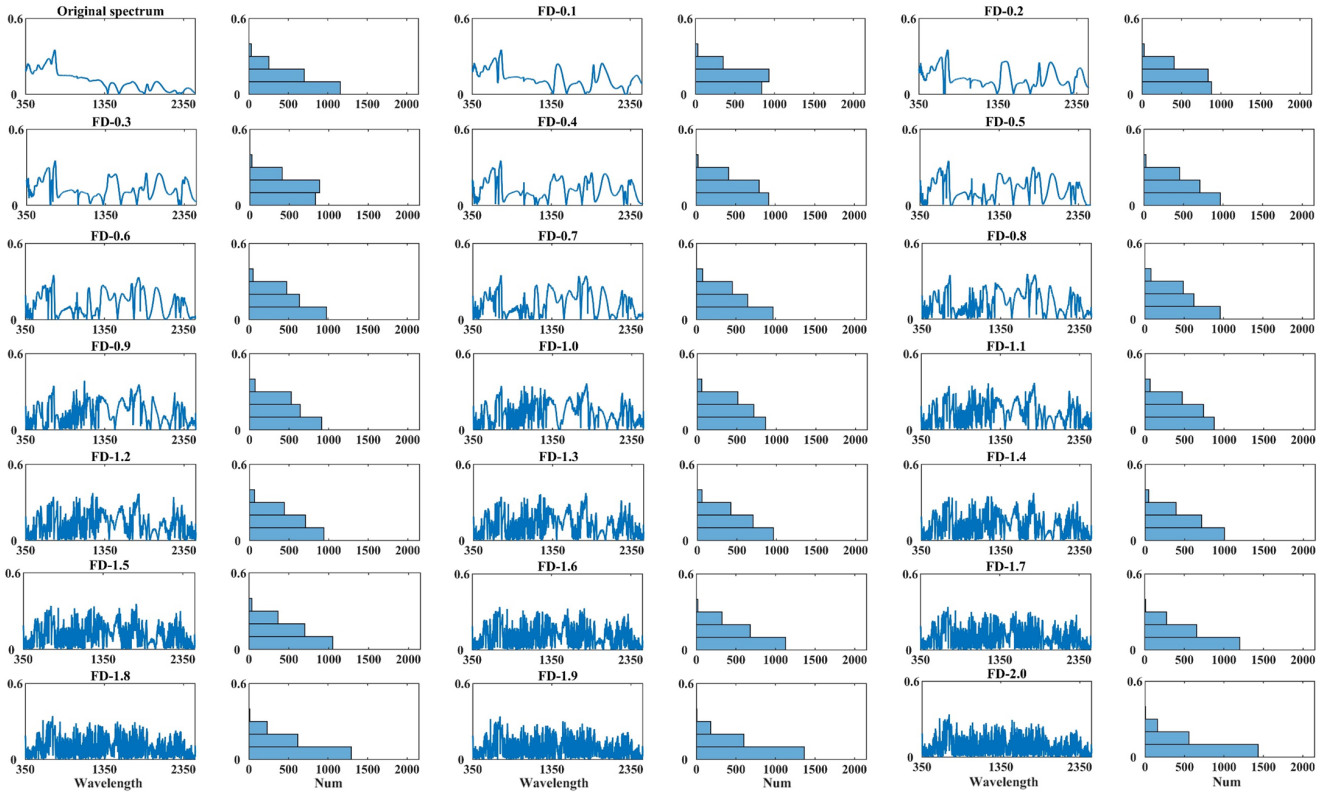


Figure 9. Pearson correlation coefficients (absolute values) of original spectrum and 0.1–2.0 order fractional differential features with malondialdehyde content and their frequency plots.

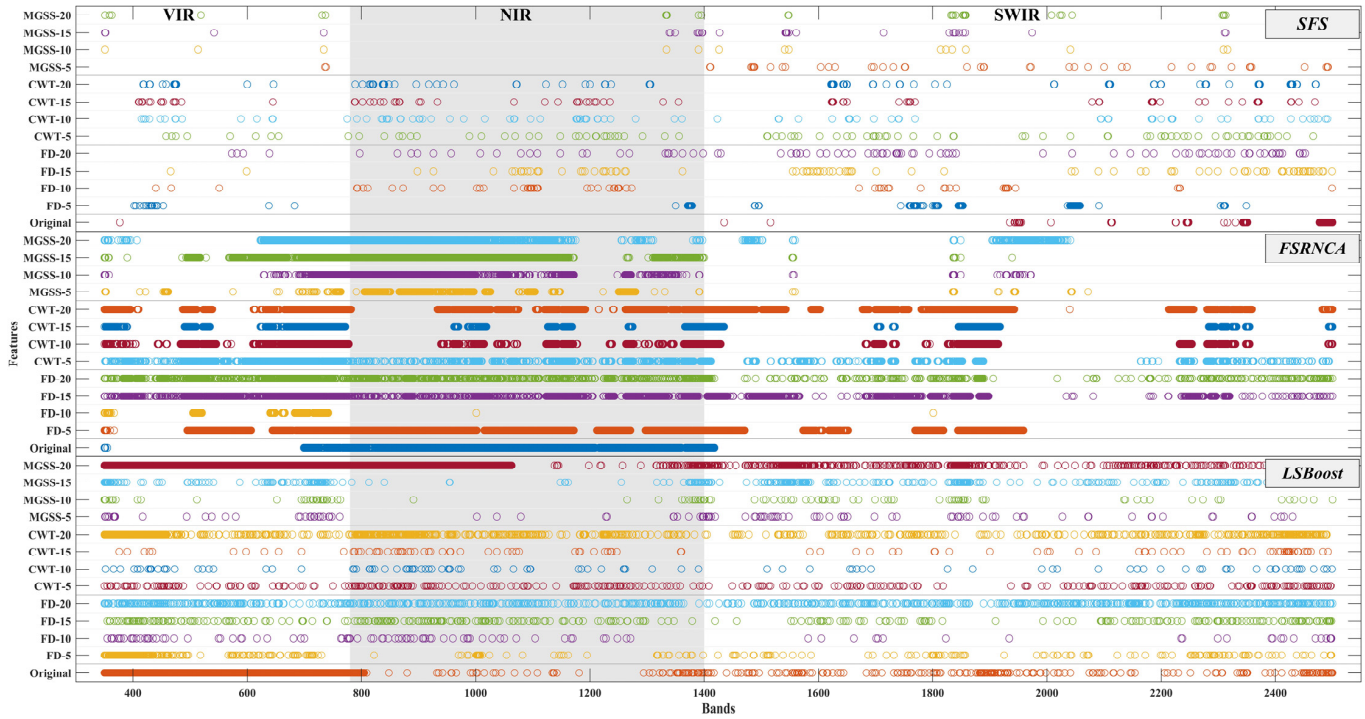


Figure 10. Distribution of model-entry features and model-entry features based on the SFS, LSBoost, and FSRNCA method for screening the original spectrum and transform features of different orders. In this paper, "original" denotes the original spectrum and "CWT-5" denotes the 5th order continuous wavelet transform.

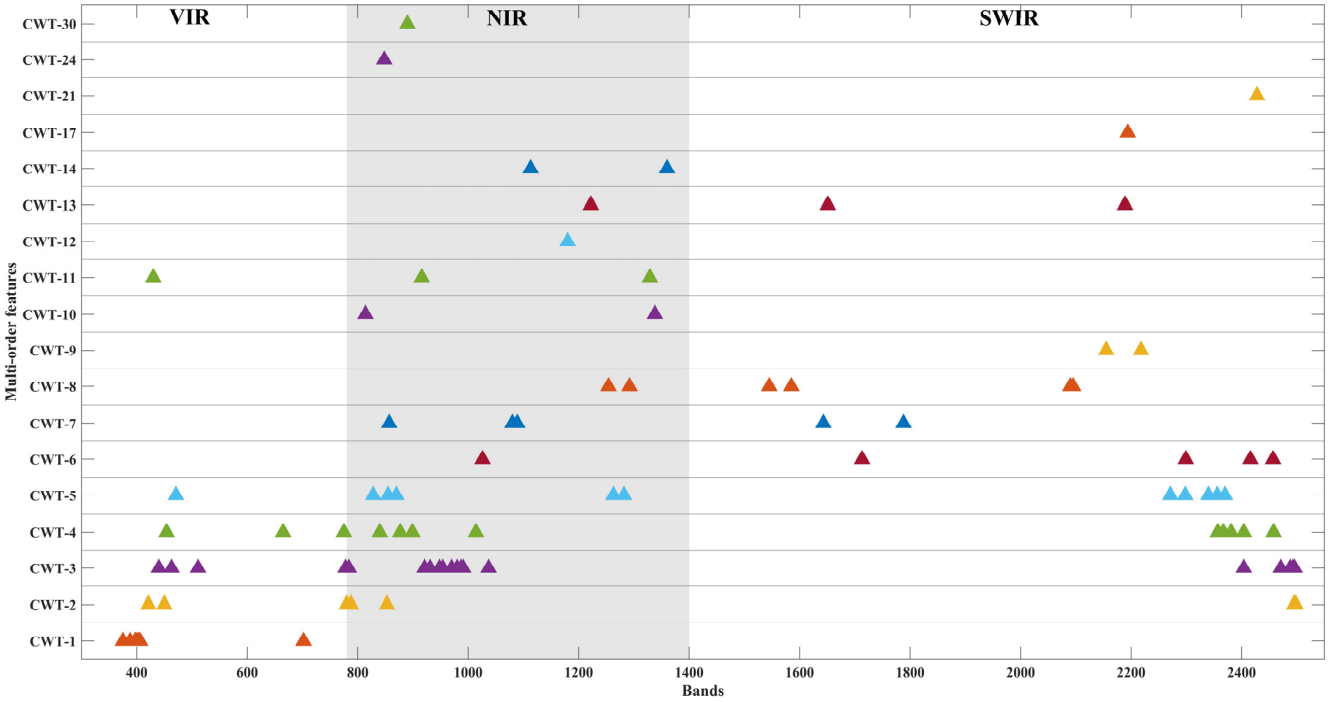


Figure 11. Combined CWT 1–30 order features selected based on the SFS method.

Table 2. The results of multi-order combination of alfalfa malondialdehyde content estimation model.

Methods	SFS				LSBoost				FSRNCA			
Characteristics	Train		Test		Train		Test		Train		Test	
	R^2	RMSE	R^2	RMSE	R^2	RMSE	R^2	RMSE	R^2	RMSE	R^2	RMSE
MGSS	0.494	28.332	0.106	36.296	0.378	31.407	0.230	33.678	0.394	30.933	0.202	34.294
FD	0.685	22.365	0.308	31.940	0.313	33.002	0.216	33.986	0.327	32.666	0.393	29.909
CWT	0.687	22.295	0.654	22.567	0.353	32.027	0.360	30.702	0.201	35.598	0.079	40.715

Figure 10 showed the selected features and distribution of the model based on the SFS, LSBoost, and FSRNCA methods for screening the original spectrum and three different orders of transformation features. From Figure 10, it can be seen that the sensitive features of the original spectrum selected based on the SFS method were mainly distributed in the 1900–2500 nm range; the sensitive features of the MGSS features were mainly distributed around 1350 nm and 1850 nm; the low-order FD features were mainly distributed around 450 nm, 1350 nm, 1750 nm, and 2080 nm and the higher-order FD features were mainly distributed in the NIR and SWIR spectrum; and the CWT features increased the sensitivities of the VIR and NIR spectrum to the MDA content, and the selected features were uniformly distributed. The sensitive features of the original spectrum selected based on the FSRNCA method were mainly distributed in the NIR; the sensitive features of the MGSS features were mainly distributed between 600 and 1400 nm; the low-order FD features were mainly distributed in the VIR and the high-order FD features were selected to have more features to yield better estimation results; and the CWT features selected based on the FSRNCA method showed aggregation in a small area range and a large range of uniform distribution.

In this paper, we screened the features based on the SFS, LSBoost, and FSRNCA method for three transform features of all order combinations, respectively, and established PLSR models. Among them, the model built based on the SFS method and 1–30 order CWT features had the best results. Figure 11 shows the model entry features screened based on the SFS method for the CWT 1–30 order combination features. They were mainly distributed in the 1st–8th orders and 9th–14th orders. The features selected in the 1st–4th

orders were mainly concentrated in the VIR and NIR of 400–1100 nm and the SWIR of 2300–2500 nm. The features selected in the 6th–8th orders were mainly concentrated in the NIR and SWIR of 1000–2200 nm.

3.3. Estimation Model of MDA Content Based on Different Order Characteristics

In this paper, we compared and analyzed the performance of screened order-by-order features (Section 3.2, Figure 10) on the PLSR model (Section 2.3.2) and assessed the estimation accuracy and precision of the model using R^2 and RMSE evaluation metrics (Section 2.3.4). As shown in Table 1, taking MGSS-5 as an example, there were three feature screening methods of SFS, LSBoost, and FSRNCA for the 5th order MGSS features, respectively, to select the sensitive features and construct the estimation model, respectively. According to the results of the evaluation indicators (Table 1), it could be found that the model based on 20-order CWT characteristics showed the lowest RMSE and the highest R^2 for the test data (R^2 = 0.430, RMSE = 28.991).

Based on the SFS method, the optimal model accuracy was 0.430 (R^2 = 0.430, RMSE = 28.991) for the test data. Compared with the original spectrum (R^2 = 0.236, RMSE = 33.563), the accuracy of the FD and CWT characteristics was improved by 0.396 times and 0.824 times, respectively, for the test data, but the accuracy of the MGSS characteristics was decreased by 0.147 times.

Based on the LSBoost method, the optimal model accuracy was 0.398 (R^2 = 0.398, RMSE = 29.783) for the test data. Compared with the original spectrum (R^2 = 0.204, RMSE = 34.258), the accuracy of the MGSS, FD, and CWT characteristics was improved by 0.265 times, 0.956 times, and 0.903 times for the test data, respectively.

Based on the FSRNCA method, the optimal model accuracy was 0.212 (R^2 = 0.212, RMSE = 37.663). Compared with the original spectrum (R^2 = 0.242, RMSE = 33.411), the accuracy of the MGSS, FD, and CWT characteristics was reduced by 0.489 times, 0.291 times, and 0.125 times, respectively.

3.4. Estimation Model of MDA Content Based on Multi-Order Combination Characteristics

In this paper, MGSS features of 1–30 order, FD features of 1–20 order, and CWT features of 1–30 order were selected and combined by SFS method, LSBoost method, and FSRNCA method to form three combined features. Taking the MGSS features of 1–30 order as an example, the MGSS-SFS combined features, MGSS-LSBoost combined features, and MGSS-FSRNCA combined features were formed, and then the estimation models were established by using three combined features. As shown in Table 2, the estimation model built using the 1–30 order CWT features screened by the SFS method was more accurate. The model test accuracy R^2 reaches 0.654 and RMSE reaches 22.567. Compared with the original spectrum, the accuracy of the MGSS, FD, and CWT characteristics was improved by 0.132 times, 0.621 times, and 1.779 times, respectively.

3.5. The Robustness of the Optimal Model

As can be seen from the graph (Figure 12) of the results of the optimal model (Section 3.4) based on multi-order combinations for predicting the test data, there was no significant deviation between the predicted and true values of the model as a whole. The alfalfa samples were divided into four parts according to the MDA content of 0–100 mmol/L, 100–150 mmol/L, 150–200 mmol/L, 200 mmol/L and above, and the performance of the comparative analytical models to estimate the performance of different contents of MDA. The MDA content was in the 150–200 mmol/L range, and the model showed some lower predictions. The MDA content in the range of 300–350 mmol/L showed outliers in the predicted values of the model.

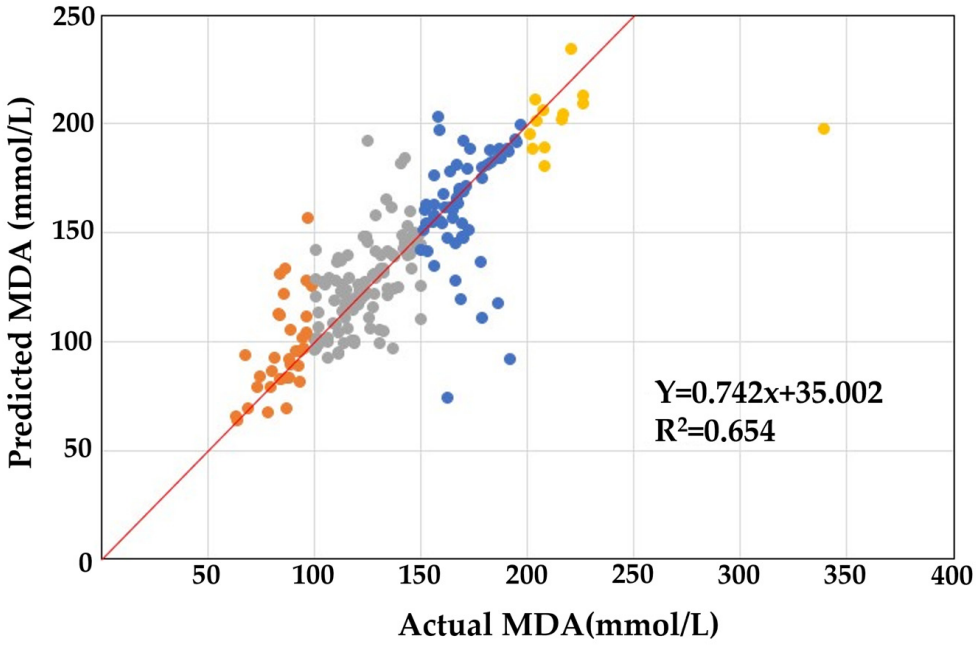


Figure 12. Scatter plots between the predicted and actual MDA content based on the prediction results of the optimal model of multi-order combination. Horizontal coordinates are real values, vertical coordinates are predicted values. The orange color indicates MDA content in the sample of 0–100 mmol/L, the gray color indicates MDA content in the sample of 100–150 mmol/L, the blue color indicates MDA content in the sample of 150–200 mmol/L, and the yellow color indicates MDA content in the sample of 200 mmol/L or more.

4. Discussion

The accurate estimation of MDA content in alfalfa tissues is a challenging task. Traditional chemical analytical methods require complex sample handling and experimental manipulation, and often result in the destruction of the sample structure [33]. In recent years, with the rapid development of spectroscopy, especially hyperspectral technology, the effective monitoring of MDA content has become feasible [14]. However, existing studies primarily utilize near-infrared hyperspectral data for MDA content estimation [13], and the potential of the full spectral range for capturing MDA content information has not been thoroughly explored. Furthermore, raw spectra are often insufficient for effectively extracting spectral information sensitive to MDA content, resulting in suboptimal model performance [34]. Spectral information enhancement technologies offer a solution by extracting hidden information and weak signals, thus improving model accuracy.

4.1. The Influencing Factors of Estimation Accuracy

In this paper, we applied various multi-order spectral transformation methods and feature selection techniques to estimate MDA content in alfalfa using the PLSR method. By analyzing the performance of the optimal models, we explored the factors influencing the estimation accuracy of different MDA content levels. A unified model was established by modeling alfalfa samples under different growth stages and salt stress conditions, reducing noise from other variables during alfalfa growth.

We compared three spectral transformation methods—CWT, FD, and MGSS—and their impact on estimation accuracy. The results showed that spectral transformation combined with appropriate feature selection significantly improved estimation accuracy. For example, the best model using the original spectrum had an R^2 of 0.209 and RMSE of 37.731, while models with spectral transformation improved accuracy by up to 1.700 times, with R^2 reaching 0.654. Among the methods, CWT showed the highest stability and accuracy, while FD and MGSS had specific advantages but also introduced noise in

certain conditions. The combination of multi-order CWT, in particular, demonstrated the ability to reduce noise, highlighting characteristic peaks and improving model accuracy. However, the characteristics of spectral transformation feature data may vary according to data sources, spectral ranges, and sample differences, which should be considered when selecting transformation methods for practical applications.

Feature selection plays a crucial role in reducing computational complexity and improving model training efficiency [35]. We compared the SFS, LSBoost, and FSRNCA methods. The results indicated that SFS outperformed other methods in terms of accuracy and robustness. SFS gradually adds relevant features, improving model generalization and interpretability while reducing overfitting and feature redundancy. Conversely, LSBoost and FSRNCA were found to be more susceptible to noise, which led to overfitting in some cases.

The robustness of the optimal model in MDA content estimation was validated through experimental results, which showed no significant deviation between the predicted and actual values. The model exhibited stable accuracy under varying salt stress conditions. However, outliers in certain data ranges, particularly above 300 mmol/L, impacted the model's accuracy due to the lack of corresponding training samples. Future studies should address these gaps by constructing a more generalized spectral database and expanding the MDA content range for broader applications.

4.2. The Advantages of Spectral Transformation Characteristics of Multi-Order Combination in MDA Estimation

The multi-order spectral transformation technique provided substantial advantages in MDA content estimation. First, it captured more comprehensive spectral information, including interactions between different wavelengths, leading to more accurate characterizations of alfalfa samples. The full wavelength model demonstrated that the most informative features were distributed across a broader spectral range than previously utilized, enhancing the reliability of MDA content estimation. Second, multi-order combinations introduced nonlinear information, which improved the model's ability to capture the complex relationships between the spectral data and MDA content. This approach significantly improved estimation accuracy compared to using the original spectrum alone.

4.3. Practical Application Value of the Proposed Method

The proposed method holds great potential for practical applications in field breeding and precision agriculture. First, it provides a non-invasive, real-time estimation tool for monitoring MDA content in alfalfa under salt stress. Since MDA is a biomarker of oxidative stress in plants, this technique offers a rapid and accurate assessment method that can aid breeders in selecting salt-tolerant varieties.

Additionally, this method is scalable and adaptable to other plant species and stress conditions, which highlights its potential for broader applications in agricultural monitoring and management. By integrating this technique into precision agriculture practices, farmers and agricultural producers can adjust management strategies based on real-time data, minimizing plant stress and maximizing crop yield and quality.

In conclusion, this study not only advances our understanding of alfalfa's growth under salt stress but also offers innovative tools for precision agriculture, contributing to the development of more sustainable and resilient agricultural systems.

5. Conclusions

In this study, we established an MDA content estimation model for *Medicago truncatula* under four distinct levels of salt stress, integrating three multi-order spectral transformation methods with three feature selection techniques. The model exhibited robust predictive capabilities for MDA content across varying salt stress conditions. The inclusion of spectral transformation features markedly enhanced estimation accuracy, with CWT features consistently surpassing both the original spectra and alternative methods, such as MGSS and

FD. Notably, among the feature selection techniques assessed, SFS emerged as the most effective for MDA content estimation. These findings highlight the significant potential of advanced spectral transformation and feature selection methodologies in improving the accuracy and reliability of MDA content estimation in alfalfa.

Author Contributions: Conceptualization, A.Z. and J.Z. (Jiaxin Zhang); methodology, A.Z. and J.Z. (Jiaxin Zhang); software, J.Z. (Jiaxin Zhang); validation, J.Z. (Jiaxin Zhang), A.Z., and J.Z. (Jingyu Zhang); formal analysis, J.Z. (Jiaxin Zhang); investigation, J.Z. (Jingyu Zhang) and X.D.; resources, A.Z. and J.Z. (Jingyu Zhang); data curation, J.Z. (Jingyu Zhang), A.Z. and J.W.; writing—original draft preparation, J.Z. (Jiaxin Zhang) and A.Z.; writing—review and editing, J.Z. (Jiaxin Zhang), J.W. and A.Z.; visualization, J.Z. (Jiaxin Zhang) and J.W.; supervision, A.Z.; project administration, A.Z.; funding acquisition, A.Z. All authors have read and agreed to the published version of the manuscript.

Funding: This research was funded by the joint program of Beijing Municipal Education Commission and Beijing Municipal Natural Science Foundation of China (KZ202110028044), the National Natural Science Foundation of China (42071303), and the Science and Technology Program of Qinghai Province of China (2022-NK-136).

Data Availability Statement: The original contributions presented in the study are included in the article, further inquiries can be directed to the corresponding author.

Conflicts of Interest: The authors declare no conflicts of interest.

References

1. Zhang, J.; Zhang, A.; Liu, Z.; He, W.; Yang, S. Multi-index fuzzy comprehensive evaluation model with information entropy of alfalfa salt tolerance based on LiDAR data and hyperspectral image data. *Front. Plant Sci.* **2023**, *14*, 1200501. [CrossRef] [PubMed]
2. Liu, D.; Bai, S.; Yang, Q.; Qi, X.; Liang, Z.; Guo, W.; Li, P. A review on the saline-alkaline tolerance of alfalfa (*Medicago sativa* L.). *J. Biol.* **2021**, *38*, 98–101+105. [CrossRef]
3. Munns, R.; Tester, M. Mechanisms of Salinity Tolerance. *Annu. Rev. Plant Biol.* **2008**, *59*, 651–681. [CrossRef]
4. Zhang, Y.; Luan, Q.; Jiang, J.; Li, Y. Prediction and Utilization of Malondialdehyde in Exotic Pine Under Drought Stress Using Near-Infrared Spectroscopy. *Front. Plant Sci.* **2021**, *12*, 735275. [CrossRef]
5. Morales, M.; Munne-Bosch, S. Malondialdehyde: Facts and Artifacts. *Plant Physiol.* **2019**, *180*, 1246–1250. [CrossRef] [PubMed]
6. Feng, M.; Guo, X.; Wang, C.; Yang, W.; Shi, C.; Ding, G.; Zhang, X.; Xiao, L.; Zhang, M.; Song, X. Monitoring and evaluation in freeze stress of winter wheat (*Triticum aestivum* L.) through canopy hyperspectrum reflectance and multiple statistical analysis. *Ecol. Indic.* **2018**, *84*, 290–297. [CrossRef]
7. Frankel, E.N.; Neff, W.E. Formation of malonaldehyde from lipid oxidation products. Biochim. Biophys. *Acta-Lipids Lipid Metab.* **1983**, *754*, 264–270. [CrossRef]
8. Chen, S.; Gao, Y.; Fan, K.; Shi, Y.; Luo, D.; Shen, J.; Ding, Z.; Wang, Y. Prediction of Drought-Induced Components and Evaluation of Drought Damage of Tea Plants Based on Hyperspectral Imaging. *Front. Plant Sci.* **2021**, *12*, 695102. [CrossRef]
9. Yuan, Z.; Tan, X. Nonlinear Screening Indicators of Drought Resistance at Seedling Stage of Rice Based on Support Vector Machine. *Acta Agron. Sin.* **2010**, *36*, 1176–1182. [CrossRef]
10. Draper, H.H.; Squires, E.J.; Mahmoodi, H.; Wu, J.; Agarwal, S.; Hadley, M. A comparative evaluation of thiobarbituric acid methods for the determination of malondialdehyde in biological materials. *Free Radic. Biol. Med.* **1993**, *15*, 353–363. [CrossRef]
11. Kong, W.; Liu, F.; Zhou, Q.; Fang, H.; He, Y. Fast Determination of Malondialdehyde in Oilseed Rape Leaves Using Near Infrared Spectroscopy. *Spectrosc. Spectr. Anal.* **2011**, *31*, 988–991. [CrossRef]
12. Sanaeifar, A.; Zhang, W.; Chen, H.; Zhang, D.; Li, X.; He, Y. Study on effects of airborne Pb pollution on quality indicators and accumulation in tea plants using Vis-NIR spectroscopy coupled with radial basis function neural network. *Ecotoxicol. Environ. Saf.* **2022**, *229*, 113056. [CrossRef] [PubMed]
13. Kong, W.; Liu, F.; Zhang, C.; Zhang, J.; Feng, H. Non-destructive determination of Malondialdehyde (MDA) distribution in oilseed rape leaves by laboratory scale NIR hyperspectral imaging. *Sci. Rep.* **2016**, *6*, 35393. [CrossRef] [PubMed]
14. Kong, W.; Liu, F.; Fang, H.; He, Y. Rapid detection of malondialdehyde in herbicide-stressed barley leaves using spectroscopic techniques. *Trans. CSAE* **2012**, *28*, 171–175. [CrossRef]
15. Shanshan, C. *Detection Method of Phenolic Compounds Content of Wine Grape Using Hyperspectral Imaging Technology During Ripening*; Northwest A&F University: Xianyang, China, 2015.
16. Cen, C.; Chu, X.; Mu, Y.; Wei, H.; Ma, Z. Non-Destructive Testing Model of Flavonoids/Polysaccharides in Anoectochilus roxburghii By Hyperspectral Imaging Technology. In Proceedings of the 2020 17th China International Forum on Solid State Lighting & 2020 International Forum on Wide Bandgap Semiconductors China (SSLChina: IFWS), Shenzhen, China, 23–25 November 2020; pp. 165–170.

17. Xie, C.; Wang, H.; Shao, Y.; He, Y. Different Algorithms for Detection of Malondialdehyde Content in Eggplant Leaves Stressed by Grey Mold Based on Hyperspectral Imaging Technique. *Int. Autom. Soft Comput.* **2015**, *21*, 395–407. [CrossRef]
18. Yao, X.; Si, H.; Cheng, T.; Jia, M.; Chen, Q.; Tian, Y.; Zhu, Y.; Cao, W.; Chen, C.; Cai, J.; et al. Hyperspectral Estimation of Canopy Leaf Biomass Phenotype per Ground Area Using a Continuous Wavelet Analysis in Wheat. *Front. Plant Sci.* **2018**, *9*, 1360. [CrossRef]
19. Li, C.; Li, X.; Meng, X.; Xiao, Z.; Wu, X.; Wang, X.; Ren, L.; Li, Y.; Zhao, C.; Yang, C. Hyperspectral Estimation of Nitrogen Content in Wheat Based on Fractional Difference and Continuous Wavelet Transform. *Agriculture* **2023**, *13*, 1017. [CrossRef]
20. Hong, Y.; Guo, L.; Chen, S.; Linderman, M.; Mouazen, A.M.; Yu, L.; Chen, Y.; Liu, Y.; Liu, Y.; Cheng, H.; et al. Exploring the potential of airborne hyperspectral image for estimating topsoil organic carbon: Effects of fractional-order derivative and optimal band combination algorithm. *Geoderma* **2020**, *365*, 114228. [CrossRef]
21. Kang, X.; Zhang, A. Hyperspectral remote sensing estimation of pasture crude protein content based on multi-granularity spectral feature. *Trans. CSAE* **2019**, *35*, 161–169. [CrossRef]
22. Fan, X.; Kang, X.; Gao, P.; Zhang, Z.; Wang, J.; Zhang, Q.; Zhang, M.; Ma, L.; Lv, X.; Zhang, L. Soil Salinity Estimation in Cotton Fields in Arid Regions Based on Multi-Granularity Spectral Segmentation (MGSS). *Remote Sens.* **2023**, *15*, 3358. [CrossRef]
23. Wang, J.; Tashpolat·Tiyip; Ding, J.; Zhang, D.; Liu, W. Estimation of desert soil organic carbon content based on hyperspectral data preprocessing with fractional differential. *Trans. CSAE* **2016**, *32*, 161–169. [CrossRef]
24. Zhang, Y.; Luo, B.; Pan, D.; Song, P.; Lu, W.; Wang, C.; Zhao, C. Estimation of Canopy Nitrogen Content of Soybean Crops Based on Fractional Differential Algorithm. *Spectrosc. Spectr. Anal.* **2018**, *38*, 3221–3230. [CrossRef]
25. Zhang, X.; He, Y.; Wang, C.; Xu, F.; Li, X.; Tan, C.; Chen, D.; Wang, G.; Shi, L. Estimation of Corn Canopy Chlorophyll Content Using Derivative Spectra in the O(2)-A Absorption Band. *Front. Plant Sci.* **2019**, *10*, 1047. [CrossRef]
26. Zhang, R.; Li, Z.; Pan, J. Coupling discrete wavelet packet transformation and local correlation maximization improving prediction accuracy of soil organic carbon based on hyperspectral reflectance. *Trans. CSAE* **2017**, *33*, 175–181. [CrossRef]
27. Kang, X.; Zhang, A. A Novel Method for High-order Residual Quantization-Based Spectral Binary Coding. *Spectrosc. Spectr. Anal.* **2019**, *39*, 3013–3020. [CrossRef]
28. Cheng, T.; Rivard, B.; Sanchez-Azofeifa, A.G.; Feret, J.B.; Jacquemoud, S.; Ustin, S.L. Predicting leaf gravimetric water content from foliar reflectance across a range of plant species using continuous wavelet analysis. *J. Plant Physiol.* **2012**, *169*, 1134–1142. [CrossRef]
29. Tian, A.; Zhao, J.; Xiong, H.; Gan, S.; Fu, C. Application of Fractional Differential Calculation in Pretreatment of Saline Soil Hyperspectral Reflectance Data. *J. Sens.* **2018**, *2018*, 8017614. [CrossRef]
30. Gnyp, M.L.; Miao, Y.; Yuan, F.; Ustin, S.L.; Yu, K.; Yao, Y.; Huang, S.; Bareth, G. Hyperspectral canopy sensing of paddy rice aboveground biomass at different growth stages. *Field Crops Res.* **2014**, *155*, 42–55. [CrossRef]
31. Becker, B.L.; Lusch, D.P.; Qi, J. Identifying optimal spectral bands from in situ measurements of Great Lakes coastal wetlands using second-derivative analysis. *Remote Sens. Environ.* **2005**, *97*, 238–248. [CrossRef]
32. Boulesteix, A.L.; Strimmer, K. Partial least squares: A versatile tool for the analysis of high-dimensional genomic data. *Brief Bioinform.* **2007**, *8*, 32–44. [CrossRef]
33. Iyengar, G.V.; Subramanian, K.S.; Woittiez, J.R.W. *Element Analysis of Biological Samples: Principles and Practices*, 1st ed.; CRC Press: Boca Raton, FL, USA, 1997; Volume II. [CrossRef]
34. Tsikas, D. Assessment of lipid peroxidation by measuring malondialdehyde (MDA) and relatives in biological samples: Analytical and biological challenges. *Anal. Biochem.* **2017**, *524*, 13–30. [CrossRef] [PubMed]
35. Man, X.; Chan, E. The best way to select features? *arXiv* **2020**. [CrossRef]

Disclaimer/Publisher's Note: The statements, opinions and data contained in all publications are solely those of the individual author(s) and contributor(s) and not of MDPI and/or the editor(s). MDPI and/or the editor(s) disclaim responsibility for any injury to people or property resulting from any ideas, methods, instructions or products referred to in the content.